Assessment of toxic potential of primary and secondary particulates/aerosols from biodiesel vis-à-vis mineral diesel fuelled engine

Article *in* Inhalation Toxicology · April 2013

DOI: 10.3109/08958378.2013.782515 · Source: PubMed

Avinash Kumar Agarwal
Indian Institute of Technology Kanpur
580 PUBLICATIONS **23,060** CITATIONS
SEE PROFILE

Tarun Gupta
Indian Institute of Technology Kanpur
345 PUBLICATIONS **23,977** CITATIONS
SEE PROFILE

Inhalation Toxicology

http://informahealthcare.com/iht
ISSN: 0895-8378 (print), 1091-7691 (electronic)

Inhal Toxicol, Early Online: 1–8

DOI: 10.3109/08958378.2013.782515

informa
healthcare

RESEARCH ARTICLE

Assessment of toxic potential of primary and secondary particulates/aerosols from biodiesel vis-à-vis mineral diesel fuelled engine

Avinash Kumar Agarwal[1], Tarun Gupta[2], Neelabh Dixit[2], and Pravesh Chandra Shukla[2]

[1]*Engine Research Laboratory, Department of Mechanical Engineering, Indian Institute of Technology Kanpur, Kanpur 208016, India and*
[2]*Department of Civil Engineering, Indian Institute of Technology Kanpur, Kanpur 208016, India*

Abstract

Toxicity of engine out emissions from primary and secondary aerosols has been a major cause of concern for human health and environmental impact. This study aims to evaluate comparative toxicity of nanoparticles emitted from a modern common rail direct injection engine (CRDI) fuelled with biodiesel blend (B20) vis-à-vis mineral diesel. The toxicity and potential health hazards of exhaust particles were assessed using various parameters such as nanoparticle size and number distribution, surface area distribution, elemental and organic carbon content and polycyclic aromatic hydrocarbons adsorbed onto the particle surfaces, followed by toxic equivalent factor assessment. It was found that biodiesel particulate toxicity was considerably lower in comparison to mineral diesel.

Keywords

Elemental and organic carbon, nanoparticles, polycyclic aromatic hydrocarbons, secondary aerosols, size and number distribution, toxicity equivalent potential

History

Received 15 January 2013
Revised 27 February 2013
Accepted 2 March 2013

Introduction

Engine exhaust is considered to be a major source of secondary organic aerosols (SOA) (Robinson et al., 2007), which has adverse effects on human health, climate, and environment (Baltensperger et al., 2008). The current vehicular emission legislations focus solely on the control of primary emissions. Currently, biodiesel is drawing serious attention globally as a part of solution to meet the demand for renewable transport fuels and to reduce greenhouse gas emissions. This calls for a comparative study of the toxic potential, quantity and nature of primary and secondary aerosols generated by a contemporary diesel engine fuelled with biodiesel blend (B20) vis-à-vis baseline mineral diesel.

The increased use of diesel engines due to their fuel economy, durability and power advantage has contributed to large volumes of diesel exhaust emissions. There is a need for clear understanding of the physicochemical nature and fate of these emissions in the environment. Diesel emissions are mainly divided into two categories: regulated emissions (nitrogen oxides, unburnt hydrocarbons, carbon monoxide and particulates) and unregulated emissions (aldehydes, benzene toulene xylene [BTX], polycyclic aromatic hydrocarbons [PAHs], etc.) (Cheung et al., 2009). Present emission regulations are based on the mass concentration of tailpipe emissions alone. However, several studies have linked the adverse health effects directly to the tiny size and overwhelmingly large number of particulates present in the diesel exhaust (Diaz et al., 2012). Therefore, there is a need to regulate the particle numbers as well in order to avoid the harmful effects of ultra fine particles. Several countries have regulated the particle number emissions in their newest emission regulations and many countries are planning to follow the suit in the near future. In the past decades, diesel emissions have been reduced greatly mainly due to advancements in combustion, engine technology, improved fuel injection systems, such as common rail direct injection (CRDI) systems, and use of exhaust gas after-treatment technologies (Majewaski and Khair, 2006). Although particulate mass emissions have reduced substantially from the modern diesel engines, particle number emissions continue to increase, which will have an important role in future emission regulations (Kittelson, 1998). Bergmann et al. (2009) observed that after-treatment devices like diesel particulate trap in the modern engines significantly decrease the total particulate mass. However, this technology increases the number concentration of nuclei mode particles downstream of filters which in-turn significantly enhances formation of SOA by providing additional surface area for condensation (Bergmann et al., 2009).

Particulate formation in diesel engine exhaust is a complex process. When the engine exhaust, volatile organic species rich in ultra fine particulates comes out of the tailpipe; it gets diluted and exhaust cooling takes place in the atmosphere. Gas-to-particle conversion of low-volatility compounds is aided by the complex free-radicals based photo-oxidation

---

Address for correspondence: Avinash Kumar Agarwal, Engine Research Laboratory, Department of Mechanical Engineering, Indian Institute of Technology Kanpur, Kanpur 208016, India. Tel/Fax: +91 512 259 7982/7408. E-mail: akag@iitk.ac.in

reactions as well as aqueous chemical oxidation processes (Kaul et al., 2011). Organic part of the particulates produced by gas-to-particle conversion is known as SOA.

Diesel engine exhaust mainly consists of elemental carbon (EC) with adsorbed vapors, a large amount of volatile and semi-volatile organic species, and a large number, and small mass of 10–50 nm diameter particles (mostly sulfate and organic carbon (OC)) formed nearly instantaneously by condensation post-combustion (Maricq, 2007). These particles are rich in many harmful organic species such as PAHs, which are carcinogenic in nature (Karavalakis et al, 2009; Ravindra et al., 2008). He et al. (2010) investigated and characterized the PAHs emissions from diesel engines. They performed the experiments using diesel, biodiesel (B100), and 20% biodiesel blend (B20). Their results showed that there was a significant reduction in PAHs emissions with B100 and B20 vis-à-vis diesel. Their analysis also showed that there was a close relationship between the emissions of PAHs and particulate matter (PM). Borras et al. (2009) conducted a study to investigate the effects of diesel reformulation on engine-operating parameters, with particular focus on PAHs emissions. There is no significant change in percentage in PAHs detection, although they used low-sulfur diesel with varying aromatic content. They concluded that PAHs emissions from the incomplete combustion of diesel greatly depend on the source of fuel and driving cycle.

In the last decade, biodiesel has emerged as an important alternative fuel for diesel engines. Biodiesel emits lesser particulate mass vis-à-vis mineral diesel and is a good alternative renewable fuel for partial replacement of mineral diesel. However, it is essential to investigate the toxicity of biodiesel exhaust particulates in primary and secondary emissions. The toxicity of these particulates largely depends on the organic fraction of the particulates. The main focus of this research is assessment of toxic potential of primary and secondary particulates/aerosols from biodiesel vis-à-vis mineral diesel-fuelled engine.

Experimental setup

Particle number, mass, and surface area distributions with respect to particle size were measured in order to physically characterize primary and secondary emissions at various engine loads (0%, 12.5%, 25%, 37.5%, 50%, 62.5%, 75%, 87.5% and 100%) for rated engine speed (1800 rpm). Chemical characterization of primary and secondary emissions was carried out using real-time EC, OC and total particle-bound PAHs measurements.

For the comparative study of mineral diesel and B20, a modern CRDI diesel engine (Tata; Safari DICOR 3.0 L) coupled with an eddy current dynamometer (Dynomerk; ECB 300) were employed. The experimental setup for this study (Figure 1) consists of a custom-built photochemical chamber. A fluorinated ethylene propylene (FEP) membrane was used to construct the chamber walls to avoid contamination and minimize wall losses. The chamber walls were transparent to complete UV spectrum. Additionally, inbetween the UV lamp banks and the photochemical chamber, a 40-μm thick sheet of cellulose acetate was used to filter out UV light with wavelengths below 300 nm (UV-C spectrum). This was done to keep the artificial light spectrum as close as possible to the spectrum of natural sunlight received at earth's surface. A humidity measurement sensor (Testo; 605H1) was used at the outlet of the photochemical chamber for monitoring temperature and humidity inside the chamber. Leak tests were performed in order to avoid any interference from the ambient. FEP membrane was thoroughly cleaned by ethanol and milli-Q water initially. Before starting an experiment, zero air supply was used to flush the photochemical chamber. Zero air supply setup comprised of an external compressor, pressure regulators, chemical scrubbers, a reactor and a temperature controller, all contained in one enclosed unit. Up to 20 LPM Zero grade air can be supplied at 4 bar pressure by the self-contained compressor. This air supply was used to flush the photochemical chamber in order to remove trace pollutants left from the previous experiment. Experimental setup was equipped with EC/OC analyzer (Sunset Laboratory; Semi-continuous field v.4) (Gupta et al., 2011); online PAHs analyzer (EcoChem Labs; PAS 2000) (Bae et al., 2004; Ott & Siegmann, 2006) to measure total particulate bound PAHs; engine exhaust particle sizer spectrometer (TSI; 3090) to measure the number-size distribution of nanoparticles (5.6–560 nm electrical mobility diameters). A partial flow dilution

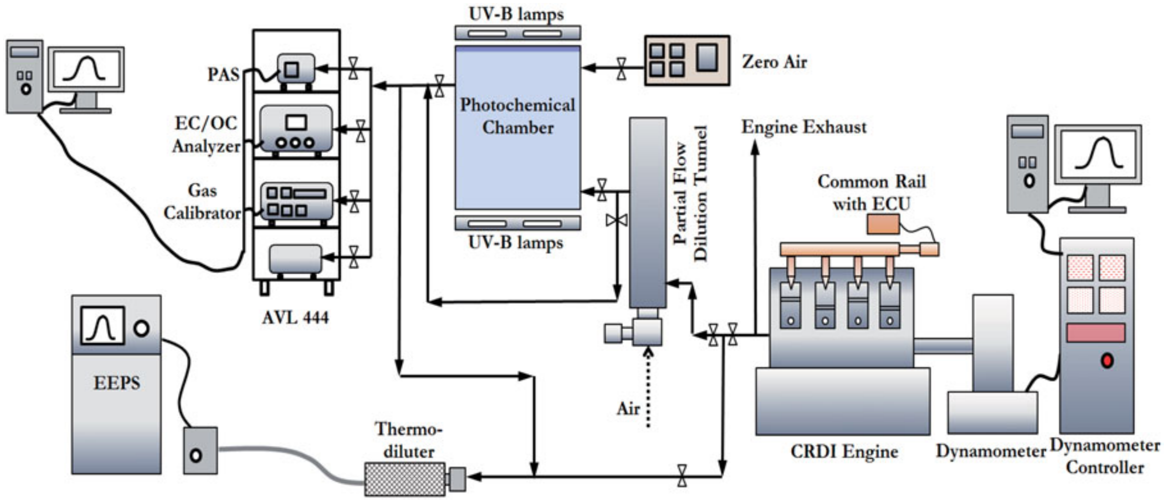

Figure 1. Schematic of the experimental setup.

tunnel was employed to dilute the engine exhaust in order to enable completion of particle formation processes mimicking atmospheric conditions (Dwivedi et al., 2006). Average wall losses (approximately 36%) were measured using the penetration of EC through the photochemical chamber in the absence of UV light. All measurements for EC, OC and total particle bound PAHs in the secondary emissions were corrected for chamber wall losses.

Physical characterization of particulates

Physical characterization of particulates was done by measurement of nanoparticle numbers, mass and surface distributions for primary and secondary aerosols at different engine loads at rated engine speed of 1800 rpm. In primary diesel exhaust, particle number concentration increased abruptly for 100% rated engine load for nucleation mode particles. For B20, there were significant number of particles less than 10 nm in the primary exhaust and the number-size distribution was relatively flatter compared to mineral diesel. It can also be noted that addition of 20% biodiesel to mineral diesel led to almost two orders of magnitude reduction in particulate size-number distribution. Most of these particles were nucleation mode particles, which usually consists of benzene soluble organic fraction (BSOF), EC and sulfates (Abdul-khalek & Kittelson, 1995). At lower engine loads, the temperature of the combustion chamber was relatively lower, which led to a large fraction of unburned fuel and lubricating oil being pyrolyzed to form a large number of nucleation mode particles (nanoparticles). As the engine load was increased, more fuel was injected in every engine cycle. Combustion takes place at relatively higher cylinder temperatures leading to more effective combustion, and lower amount of unburnt organic species were produced in the cylinder. This led to reduction in BSOF of the particulates and higher exhaust gas temperatures resulted in a phase transition, increasing their concentration in the gas phase. This also led to reduction in total number of particles emitted with increasing engine load as BSOF is critical for growth of soot nuclei. Similarly, sulfur content of the fuel dictates the number of sulfate nuclei formed in the cylinder. This further explains lower number concentration of primary particles from B20 as biodiesel is essentially sulfur free. Biodiesel also contains approximately 10% (w/w) oxygen, which leads to sharp reduction in particle number-size distribution in the primary exhaust.

There was a sharp decrease in particle number concentration in secondary aerosols in comparison to the primary emissions (Figure 2). This might be possibly due to gravitational settling, wall losses, sampling losses and various other chemical reactions occurring inside the photo-chemical chamber (Gupta et al., 2011; Ruiz et al., 2007). Significantly lower particle number concentration in secondary emissions was observed for no load for both the fuels. A large number of smaller particles emitted (particularly at lower engine loads) enter the photochemical chamber, undergo condensational growth and agglomeration. These processes result in lower number concentrations and increase in particle diameters. However, it is interesting to note that very small particles (<10 nm) emitted by B20 were still prevailing as secondary aerosols. Particles emitted (in primary emissions) at higher engine loads were dominated by relatively larger particles, which shows slightly lower tendency to undergo agglomeration.

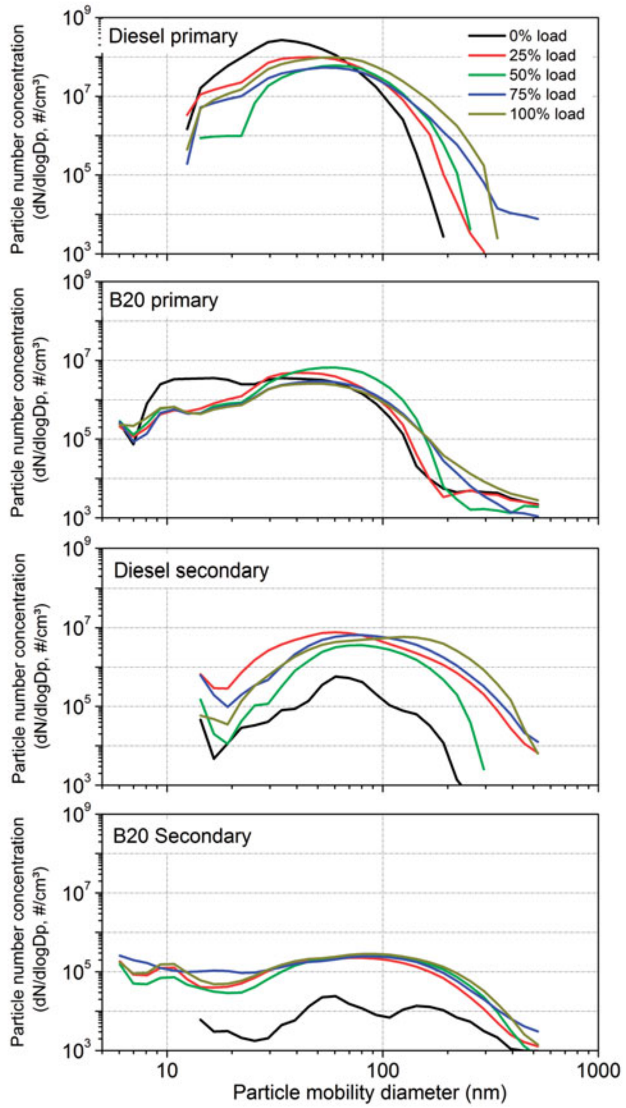

Figure 2. Particle number concentration versus mobility diameter for primary and secondary exhaust fuelled with diesel and B20.

A sudden increase in number concentration was observed at 25% engine load for both the fuels. Possibly, the conditions inside the photochemical chamber (37.5 °C and 50% RH) might be the most favorable for SOA formation. Peaks were also observed in the particle number concentration in secondary emissions at smaller particle diameters, which is more clearly visible in secondary emissions from B20. This is a sign of fresh nuclei formation in the photochemical chamber, which is in line with the observations of Robinson et al. (2007). The particles inside the chamber were in a heterogeneous transient phase. This also explains high variability in the aerosol size distribution for the secondary aerosols.

As the engine load increased, the peak of particle number concentration shifted toward larger diameters for primary as well as secondary aerosols for both fuels. The particle number

Figure 3. Integrated particulate matter (PM) mass and surface area concentrations versus engine load for primary and secondary exhaust fuelled with diesel and B20.

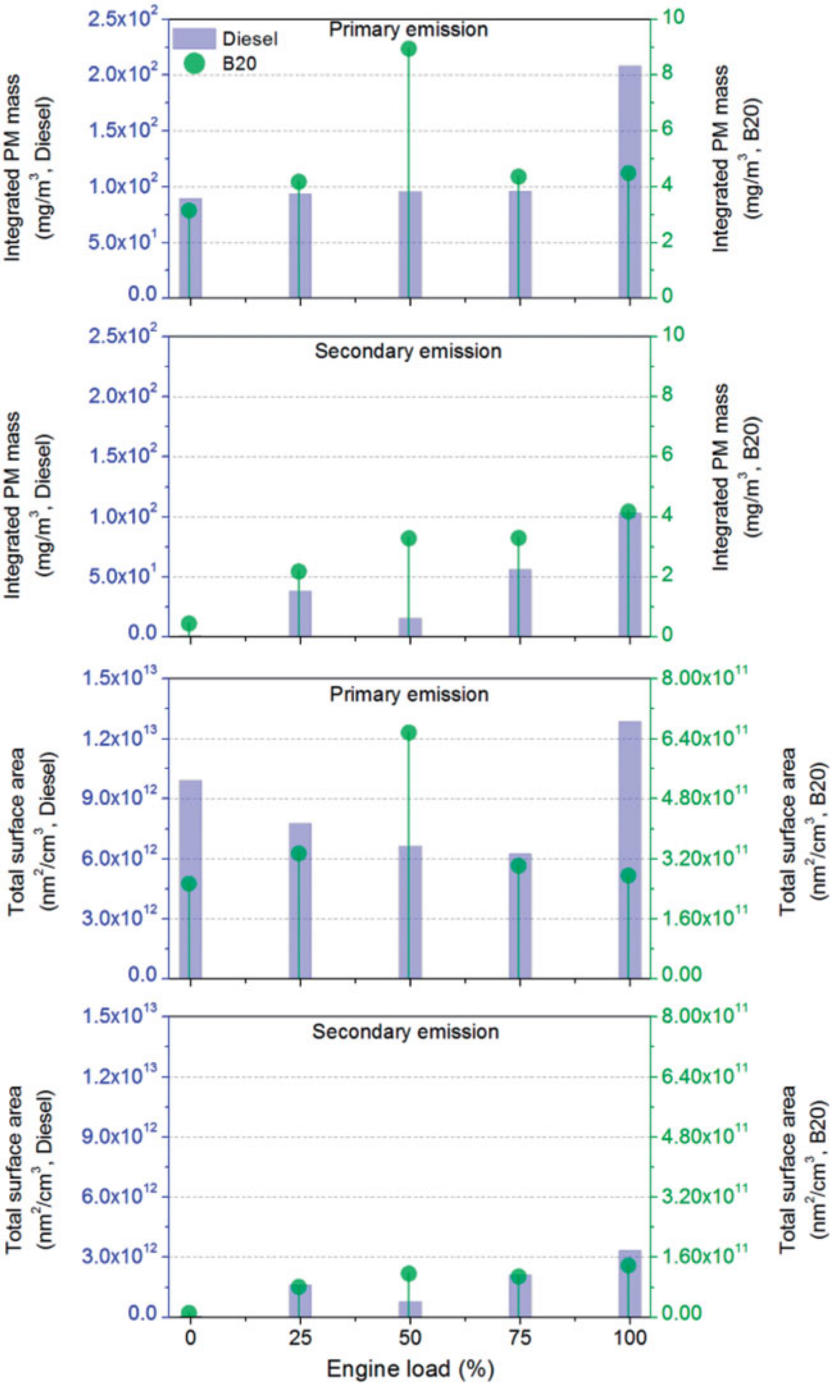

concentration in primary and secondary diesel exhaust was an order of magnitude higher than B20 (Agarwal et al., 2011).

At a constant rated engine speed of 1800 rpm, the total PM mass in primary emissions from diesel increases with engine load (Figure 3). Particle number concentrations at lower engine loads were higher, but particle diameters were smaller. Hence, they cannot contribute significantly to the PM mass. For B20, at lower engine loads, PM mass in the primary emissions increased with engine load, with a maxima at 50% engine load. The PM mass in primary and secondary emissions from diesel was higher than B20 by an order of magnitude. Numerous studies in the literature have indicated similar trends (Agarwal et al., 2011; Cowley et al., 1993; Den Ouden et al., 1994; Kalligeros et al., 2003; Lange, 1991). Oxygen content of B20 favors efficient fuel combustion resulting in the lower PM mass (Akasaka et al., 1997; American Biofuels Association, 1995; Owen & Coley, 1995).

Total surface area of the particles would be directly proportional to the particle's number and inversely proportional to the particle size. Reduction in primary emission particle number concentration and increase in the particle size were observed with increasing engine load for B20. Higher number concentration at lower engine loads (Figure 2) for primary diesel emissions leads to lower PM mass and higher particulate surface area (Figure 3). For B20, the trend of particulate surface area curve is very well correlated to the PM mass curve, with a peak at 50% engine load. At 100% engine load, i.e. rated engine load, the mode of number-size distribution (Figure 2) shifts toward right and the area under the curve is maximum, which results in the maximum particle

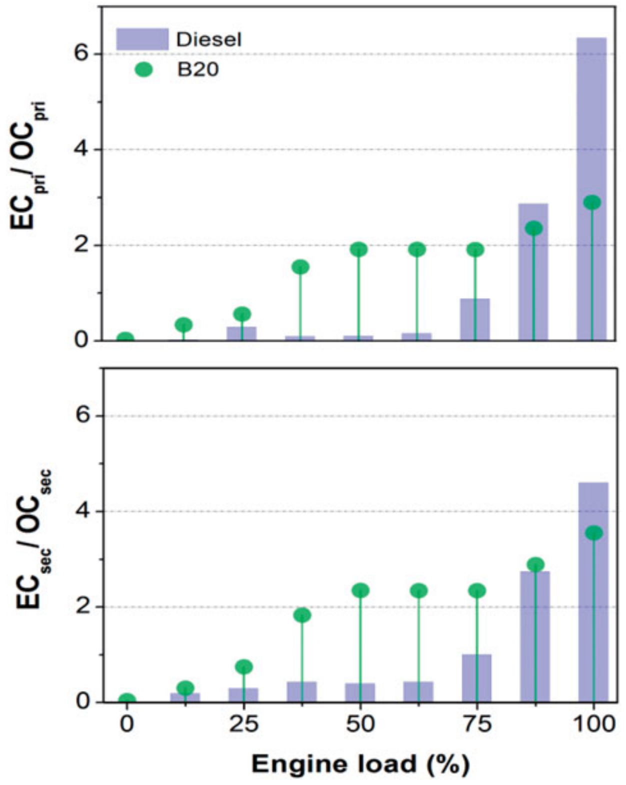

Figure 4. Variation of EC/OC ratio for primary and secondary versus engine load for primary and secondary exhaust fuelled with diesel and B20.

surface area for primary diesel emissions (Figure 3). At all engine loads, the surface area distribution in primary emissions from diesel is an order of magnitude higher than B20.

Chemical characterization of particulates

Increase in particle number concentration in secondary emissions (Figure 2) with increase in engine load was the main reason for corresponding increase in particulate surface area (Figure 3). The surface area distribution in secondary emissions from diesel was higher by an order of magnitude compared to B20. Larger surface area of particles provided more sites for condensation of toxic organic species (Bruske et al., 2010). Therefore, secondary emissions from diesel would have higher toxic potential compared to B20.

The trend of increase in EC upon increasing engine load matches with the variation of EC with engine load, as observed in a recent study on secondary OC from mineral diesel fuelled CRDI engine (Gupta et al., 2011). At higher engine loads, the fuel-to-air ratio and the temperature of the combustion chamber, both were relatively higher leading to higher EC formation. Moreover, at very high engine loads, relatively higher temperatures caused lubricating oil pyrolysis resulting in even higher EC (Sharma et al., 2005).

OC fraction mainly comprises of unburnt fuel, lubricating oil, and products of incomplete combustion. At lower engine loads, OC increased with an increase in engine load until it attained maxima. From here, it started decreasing with further increase in engine load (Gupta et al., 2011). Higher oxygen content of B20 facilitated more efficient combustion vis-à-vis mineral diesel. This brought about a relative reduction in the unburned hydrocarbon content (primarily OC) of B20 particulates therefore a higher EC/OC ratio was observed for primary as well as secondary particles (Figure 4). The EC/OC ratio was found to be higher for diesel at relatively higher engine loads. This could be possibly because of a more pronounced peak of OC observed at 50% engine load. For B20, EC/OC ratio was relatively lower compared to diesel at higher engine loads.

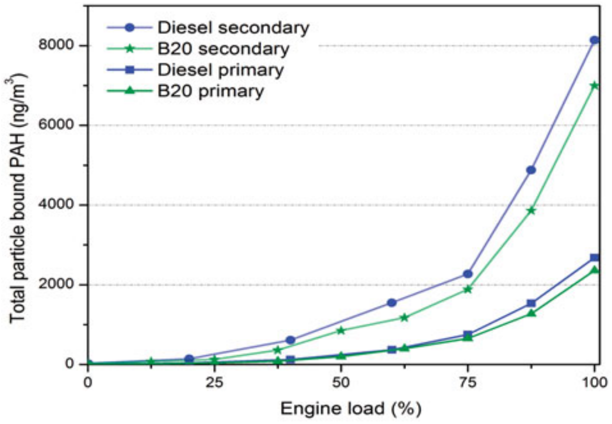

Figure 5. Variation of total particle-bound PAHs versus engine load for primary and secondary exhaust fuelled with diesel and B20.

At a constant engine speed of 1800 rpm, the total particle bound PAHs increase with an increase in engine load (Figure 5) for both fuels. PAHs in secondary emissions were higher than primary emissions at all engine loads for both fuels. At higher engine loads, high cylinder temperature facilitates cyclization of unburned fuel and lubricating oil, leading to formation of PAHs by pyrosynthesis (Ravindra et al., 2008). As a result of cooling and aging processes, large amount of gaseous phase PAHs undergo phase transition and condense onto the particulates. PAHs get adsorbed onto the exhaust particles and somehow persist as a result of incomplete combustion inside the engine (Atal et al., 1997). One interesting observation is that there was a drastic reduction in PM mass for B20 vis-à-vis diesel, whereas particle bound PAHs were comparable for both the fuels. This indicates that the particulates from B20 were relatively highly loaded with PAHs.

PAHs and nitro-PAHs speciation and determination of toxic equivalent factor

PAHs are categorized as one of the major carcinogenic compounds in the environment, which are formed by incomplete combustion of fuels in combustion systems. PAHs are mainly composed of hydrogen and carbon with traces of oxygen but sometimes may also contain nitrogen, and such species are called nitro-PAHs, which are highly toxic in nature. The toxic properties of PAHs are highly dependent on its molecular structure. Several studies show that some PAHs are highly toxic but on the other hand, some of them are relatively benign (Ravindra et al., 2008). Determination of toxic potential of PAHs can be evaluated for understanding the toxic impacts produced by individual species of PAHs. This can be determined by integrating the individual toxicity of PAHs, which can be obtained by

Table 1. Total toxic potential calculation of individual PAHs for diesel (primary and secondary emissions).

			Engine load (%)						
S No.	PAHs	TEFs	0	20	40	60	75	87.5	100
Toxic potential calculation for primary emissions (diesel)									
1	B[A]A	0.1	0.055	0.405	1.274	3.828	7.749	15.861	27.759
2	CHR	0.01	0.010	0.076	0.240	0.722	1.462	2.992	5.236
3	B[B]F	0.1	0.071	0.520	1.638	4.923	9.966	20.401	35.704
4	B[K]F	0.1	0.065	0.479	1.509	4.534	9.178	18.788	32.882
5	B[A]P	1	0.439	3.232	10.176	30.579	61.903	126.715	221.767
6	I[1,2,3]P	0.1	0.079	0.578	1.821	5.473	11.079	22.679	39.691
7	D[A,H]A	1.1	0.203	1.495	4.707	14.143	28.631	58.608	102.571
8	B[G,H,I]P	0.01	0.008	0.061	0.191	0.573	1.159	2.373	4.153
	N-PAHs								
9	1-NPYR	0.1	0.013	0.094	0.296	0.888	1.798	3.681	6.441
10	6-NCHR	10	0.067	0.492	1.548	4.652	9.418	19.279	33.740
Total toxic potential			1.010	7.432	23.399	70.314	142.344	291.377	509.944
Toxic potential calculation for secondary emission (diesel)									
1	B[A]A	0.1	0.264	1.442	6.304	16.029	23.495	50.472	84.235
2	CHR	0.01	0.050	0.272	1.189	3.023	4.432	9.520	15.888
3	B[B]F	0.1	0.339	1.854	8.108	20.616	30.219	64.917	108.342
4	B[K]F	0.1	0.312	1.708	7.467	18.987	27.831	59.786	99.779
5	B[A]P	1	2.107	11.518	50.359	128.053	187.702	403.220	672.948
6	I[1,2,3]P	0.1	0.377	2.061	9.013	22.918	33.594	72.167	120.442
7	D[A,H]A	1.1	0.974	5.327	23.292	59.227	86.816	186.496	311.250
8	B[G,H,I]P	0.01	0.039	0.216	0.943	2.398	3.515	7.551	12.603
	N-PAHs								
9	1-NPYR	0.1	0.061	0.335	1.463	3.719	5.452	11.712	19.546
10	6-NCHR	10	0.321	1.752	7.662	19.482	28.558	61.347	102.385
Total toxic potential			4.845	26.485	115.798	294.453	431.614	927.188	1547.418

Table 2. Total toxic potential calculation of individual PAHs for B20 (primary and secondary emissions).

			Engine load (%)								
S No.	PAHs	TEFs	0	12.5	25	37.5	50	62.5	75	87.5	100
Toxic potential calculation for primary emission(B20)											
1	B[A]A	0.1	0.077	0.211	0.602	1.115	2.761	5.516	9.108	17.703	32.770
2	CHR	0.01	0.012	0.033	0.094	0.175	0.433	0.864	1.427	2.773	5.133
3	B[B]F	0.1	0.067	0.184	0.527	0.975	2.414	4.823	7.964	15.479	28.653
4	B[K]F	0.1	0.074	0.203	0.581	1.075	2.663	5.319	8.783	17.070	31.599
5	B[A]P	1	0.323	0.885	2.530	4.681	11.596	23.165	38.250	74.342	137.617
6	I[1,2,3]P	0.1	0.065	0.179	0.511	0.946	2.343	4.680	7.729	15.021	27.806
7	D[A,H]A	1.1	0.226	0.619	1.771	3.276	8.117	16.215	26.775	52.040	96.332
8	B[G,H,I]P	0.01	0.007	0.020	0.056	0.104	0.257	0.513	0.847	1.646	3.047
	N-PAHs										
9	1-NPYR	0.1	0.025	0.069	0.197	0.364	0.901	1.800	2.973	5.777	10.695
10	6-NCHR	10	0.018	0.049	0.141	0.261	0.646	1.291	2.131	4.142	7.668
Total toxic potential			0.895	2.452	7.010	12.969	32.132	64.186	105.987	205.994	381.320
Toxic potential calculation for secondary emission (B20)											
1	B[A]A	0.1	0.319	1.054	1.751	4.972	11.813	16.292	26.170	53.635	97.191
2	CHR	0.01	0.050	0.165	0.274	0.779	1.851	2.552	4.099	8.402	15.225
3	B[B]F	0.1	0.279	0.921	1.531	4.348	10.329	14.245	22.882	46.898	84.982
4	B[K]F	0.1	0.308	1.016	1.688	4.795	11.391	15.710	25.235	51.720	93.720
5	B[A]P	1	1.340	4.426	7.353	20.881	49.610	68.418	109.900	225.241	408.155
6	I[1,2,3]P	0.1	0.271	0.894	1.486	4.219	10.024	13.824	22.206	45.511	82.469
7	D[A,H]A	1.1	0.938	3.098	5.147	14.617	34.727	47.893	76.930	157.669	285.709
8	B[G,H,I]P	0.01	0.030	0.098	0.163	0.462	1.098	1.515	2.433	4.987	9.037
	N-PAHs										
9	1-NPYR	0.1	0.104	0.344	0.571	1.623	3.855	5.317	8.541	17.504	31.719
10	6-NCHR	10	0.075	0.247	0.410	1.163	2.764	3.812	6.123	12.550	22.742
Total toxic potential			3.714	12.263	20.375	57.859	137.464	189.578	304.520	624.116	1130.949

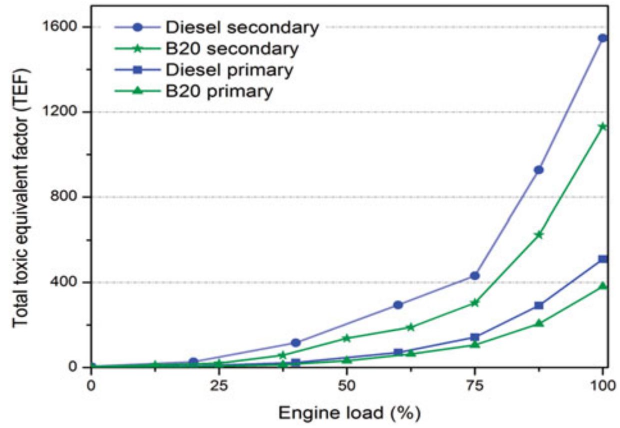

Figure 6. Values of total toxic equivalent potentials with respect to engine load for primary and secondary exhaust fuelled with diesel and B20.

multiplying the toxic equivalent factors (TEFs) of the individual PAH species with their respective concentrations. TEFs for PAHs were obtained from the study conducted by Nisbet & Lagoy (1992) and are also reported by CAEPA (1993). In this study, a total of eight PAHs and two nitro-PAHs were considered for the evaluation of toxic potential.

Pan et al. (1998) compared the PAHs and nitro-PAHs emissions from diesel, biodiesel (B100; soy methyl ester), and B20. They performed experiment on a Cummins B5.9 engine. The values for PAHs and nitro-PAHs emissions for diesel as well as biodiesel blends were obtained by using gas chromatography and mass spectrometry. In our calculations, the data for percentage distribution of PAHs species from the study of Pan et al. (1998) have been used. Total PAHs data in this study is attributed to individual PAHs based on the above study.

The trend of total toxic equivalent potential (Figure 6) was similar to particle-bound PAHs emissions (Figure 5). Diesel showed slightly higher toxic potential compared to B20 for both primary and secondary particles. Primary particles have lesser total toxic potential compared to secondary particles. When exhaust emanates from the exhaust pipe, a major part of PAHs are present in vapor phase, which remain undetected during primary particle phase PAHs measurement. In this study, secondary measurements were taken after 2 h photochemical chamber residence time. This provided sufficient time for the condensation and transformation of gas phase aged PAHs into particle bound PAHs.

It was observed that TEFs for diesel was higher at 100% engine load for both primary and secondary particles. Overall TEFs were 509.944 and 381.32 for diesel and B20 (primary particles), respectively, at 100% engine load. Similarly, TEFs were 1547.42 and 1130.35 for diesel and B20 (secondary particles), respectively, at 100% engine load. The lower values of TEFs for B20 indicate that it predominantly has individual PAHs with lower toxicity. This signifies that, although B20 originated particulates had significantly higher PAHs loading, their contribution to overall toxicity was far lesser than that of particulates from mineral diesel. Details about TEFs for both fuels (primary and secondary particulates both) are given in tabular form in Tables 1 and 2.

Conclusions

In this study, particle number emissions, PM mass emissions, EC/OC and PAHs emissions were compared for diesel and B20. Lower BSOF in the exhaust particulates were found at higher engine loads. As the engine load increased, BSOF content of the particulates decreased and there was a phase transition enriching their concentration in the gas phase. This led to reduction in number of particles emitted with increasing engine load because BSOF was critical for particulate growth. Particle number-size distribution peak shifted toward right side on the particle size axis for secondary emissions for both fuels (diesel and B20). Particle number concentration was two orders of magnitude lower for biodiesel blend for primary as well as secondary emissions. The amount of sulfur in the fuel primarily dictates the sulfate nuclei formation. This explains lower number of primary particles in B20 exhaust since biodiesel is essentially sulfur free. Total PM mass was also an order of magnitude lower for B20 exhaust for primary as well as secondary emissions. For B20, EC/OC ratio was relatively lower compared to diesel at higher engine loads. PAHs were significantly higher in secondary emissions for both fuels. The gas-to-particle phase conversion of PAHs in the exhaust leads to higher concentration of PAHs in the secondary emissions. PAHs were higher in case of diesel for both primary and secondary particulates. The particulates emitted by B20 were laden with PAHs to a higher degree. Toxicity was found to be higher for secondary particles compared to primary particles for both the fuels. Toxicity was also found to be lower for B20 in both primary and secondary particles vis-à-vis mineral diesel. The lower value of total toxicity for B20 indicates that it predominantly has individual PAHs with lower toxicity. This concludes that although B20 originated particulates have significantly higher PAHs loading, their contribution to overall toxicity is far lesser than that of particulates from mineral diesel.

Acknowledgements

The expert group of DST TSG made very valuable comments, which helped in addressing some important issues successfully.

Declaration of interest

The authors gratefully acknowledge the generous funding from Technology Systems Group (TSG) of Department of Science and Technology (DST), Government of India for carrying out this study (Grant ID: DST/TSG/AF/2007/21).

References

Abdul-khalek IS, Kittelson DB. (1995). Real time measurement of volatile and solid exhaust particles using a catalytic stripper. SAE Paper No. 950236.

Agarwal AK, Gupta T, Kothari A. (2011). Particulate emissions from biodiesel vs. diesel fuelled compression ignition engine. Renew Sustain Energy Rev 15:3278–300.

Akasaka Y, Suzuki T, Sakurai Y. (1997). Exhaust emissions of a DI diesel engine fueled with blends of biodiesel and low sulfur diesel fuel. SAE Paper no. 972998.

American Biofuels Association. (1995). The biodiesel industry in the United States: an industry on the move. An update. Arlington: ABA.

Atal A, Levendis YA, Carlson J, et al. (1997). On the survivability and pyrosynthesis of PAH during combustion of pulverized coal and tire crumb. Combust Flame 110:462–78.

Bae MS, Schauer JJ, DeMinter JT, et al. (2004). Validation of a semi-continuous instrument for elemental carbon and organic carbon using a thermal-optical. Atmos Environ 38:2885–93.

Baltensperger U, Dommen J, Alfarra MR, et al. (2008). Combined determination of the chemical composition and health effects of secondary organic aerosols: the POLYSOA project. J Aerosol Med Pulm Drug Deliv 21:145–54.

Bergmann M, Kirchner U, Vogt R, et al. (2009). On-road and laboratory investigation of low-level pm emissions of a modern diesel particulate filter equipped diesel passenger car. Atmos Environ 43:1908–16.

Borras E, Tortajada LA, Vazquez M, et al. (2009). Polycyclic aromatic hydrocarbon exhaust emissions from different reformulated diesel fuels and engine operating conditions. Atmos Environ 43:5944–52.

Bruske I, Hampel R, Socher MM, et al. (2010). Impact of ambient air pollution on the differential white blood cell count in patients with chronic pulmonary disease. Inhal Toxicol 22:245–52.

CAEPA. (1993). Benzo[a]Pyrene as a toxic contaminant. Part B: health assessment. California: Environmental Protection Agency.

Cheung CS, Zhu L, Huang Z. (2009). Regulated and unregulated emissions from a diesel engine with biodiesel and biodiesel with methanol. Atmos Environ 43:4865–72.

Cowley LT, Stradling RJ, Doyon J. (1993). The influence of composition and properties of diesel fuel on particulate emissions from heavy-duty engines. SAE Paper no. 932732.

Den Ouden CJJ, Clark RH, Cowley LT, et al. (1994). Fuel quality effects on particulate matter emissions from light-and heavy-duty diesel engines. SAE Technical Paper 942022.

Diaz EA, Chung Y, Papapostolou V, et al. (2012). Effects of fresh and aged vehicular exhaust emissions on breathing pattern and cellular responses-pilot single vehicle study. Inhal Toxicol 24:288–95.

Dwivedi D, Agarwal AK, Sharma M. (2006). Particulate emission characterization of a biodiesel vs. diesel-fuelled compression ignition transport engine: a comparative study. Atmos Environ 40:5586–95.

Gupta T, Dixit N, Agarwal AK. (2011). The secondary organic carbon (SOC) formation from a CRDI automotive diesel engine exhaust. SAE Paper no. 2011-01-0642.

He C, Ge Y, Tan J, et al. (2010). Characteristics of polycyclic aromatic hydrocarbons emissions of diesel engine fueled with biodiesel and diesel. Fuel 89:2040–6.

Kalligeros S, Zannikos F, Stournas S, et al. (2003). An investigation of using biodiesel/marine diesel blends on the performance of a stationary diesel engine. Biomass Bioenergy 24:141–9.

Karavalakis G, Stournas S, Bakeas E. (2009). Effects of diesel/biodiesel blends on regulated and unregulated pollutants from a passenger vehicle operated over the European and the Athens driving cycles. Atmos Environ 43:1745–52.

Kaul DS, Gupta T, Tripathi SN, et al. (2011). Secondary organic aerosol: a comparison between foggy and nonfoggy days. Environ Sci Technol 45:7307–13.

Kittelson DB. (1998). Engines and nanoparticles: a review. J Aerosol Sci 29:575–88.

Lange WW. (1991). The effect of fuel properties on particulates emissions in heavy-duty truck engines under transient operating conditions. Technical report, Society of Automotive Engineers.

Majewaski WA, Khair MK. (2006). Diesel emissions and their control. Warrendale, PA: SAE International.

Maricq MM. (2007). Chemical characterization of particulate emissions from diesel engines: a review. Aerosol Sci 38:1079–118.

Nisbet IC, Lagoy PK. (1992). Toxic equivalency factors (TEFs) for polycyclic aromatic hydrocarbons (PAHs). Regulat Toxicol Pharmacol 16:290–300.

Ott WR, Siegmann HC. (2006). Using multiple continuous fine particle monitors to characterize tobacco, cooking, wood burning and vehicular sources in indoor. Atmos Environ 40:821–43.

Owen K, Coley T. (1995). Automotive fuels reference book. Warrendale, PA: SAE International.

Pan J, Quarderer S, Smeal T, et al. (1998). Comparison of PAH and nitro-PAH emissions among standard diesel fuel, biodiesel fuel, and their blend on diesel engines. Proceedings of the 46th ASMS Conference on Mass Spectrometry and Allied Topics, pp. 370.

Ravindra R, Sokhi R, Grieken RV. (2008). Atmospheric polycyclic aromatic hydrocarbons: source attribution, emission factors and regulation. Atmos Environ 42:2895–921.

Robinson AL, Donahue NM, Shrivastava MK, et al. (2007). Rethinking organic aerosols: semi volatile emissions and photochemical aging. Science 315:1259–62.

Ruiz PA, Lawrence JE, Wolfson JM, et al. (2007). Development and evaluation of a photochemical chamber to examine the toxicity of coal-fired power plant emissions. Inhal Toxicol 19:1–10.

Sharma M, Agarwal AK, Bharathi KVL. (2005). Characterization of exhaust particulates from diesel engine. Atmos Environ 39: 3023–8.